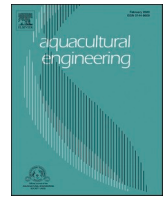




Contents lists available at ScienceDirect

Aquacultural Engineering

journal homepage: www.elsevier.com/locate/aque

Steady-state and dynamic model for recirculating aquaculture systems with pH included

Allyne M. dos Santos^a, Lucas F. Bernardino^a, Kari J.K. Attramadal^{b,c}, Sigurd Skogestad^{a,*}

^a Department of Chemical Engineering, Norwegian University of Science and Technology (NTNU), Sem Sælandsvei 4, Kjemiblokk 5, 101B, Trondheim 7491, Norway

^b Department of Research and Development, Nofitech AS, Dyre Halses gate 18, Trondheim 7042, Norway

^c Department of Biotechnology and Food Science, Norwegian University of Science and Technology (NTNU), Sem Sælandsvei 6–8, Kjemiblokk 3, 163, Trondheim 7491, Norway

ARTICLE INFO

Keywords:

First-principle modelling
Recirculating Aquaculture Systems
pH modelling

ABSTRACT

In this work, simplified steady-state and dynamic models of a Recirculating Aquaculture System (RAS) of Atlantic salmon (*Salmo salar*) are described. The RAS process under study includes a fish tank, a biofilter, a CO₂ stripper, and an oxygen cone. Compared to existing models, the main contribution is that it explicitly models the pH, by using reaction invariants such as total inorganic carbon (TIC), total ammonia nitrogen (TAN), and alkalinity. As the possibility of placing the pH/alkalinity adjustment (base or buffer addition) into the fish tank or into the biofilter was considered, four steady-state scenarios were studied, where one of the adjustments is utilized in each scenario. A dynamic simulation of the process with oxygen and pH controllers was performed and compared with commercial RAS production data, and what adjustments had to be done to get an agreement between the model and the plant data.

1. Introduction

Fish aquaculture involves the use of large tanks filled with freshwater or saltwater to cultivate fish. As the global demand for food continues to grow, the Food and Agriculture Organization of the United Nations (FAO) has recognized aquaculture as a promising source of food to meet this demand (FAO, 2020).

Atlantic salmon undergo freshwater stages until they reach a mature smolt size, after which they are transferred to net pens during the post-smolt phase and continue to grow until they reach market size (Global Salmon Initiative, 2020). Expanding the inland phase of aquaculture has several advantages, including reducing fish losses from escapes, lowering the probability of diseases due to the absence of contact with external pathogens, and the ability to provide controlled rearing conditions with vaccinations. However, the main disadvantage is that as the fish grow, they require more space and may need to be spread across multiple tanks or transferred to larger tanks on land.

The current types of configuration of recirculating aquaculture systems (RAS) show room for improvement, as they are not operated optimally and are not fully automated, i.e., they are operated manually to preserve satisfactory conditions for the welfare of the fish.

There is room for improvement in the current configuration of

recirculating aquaculture systems (RAS) as they are not operated optimally and lack full automation. Instead, they are manually operated to maintain satisfactory conditions for the fish's welfare.

Carbon dioxide (CO₂), ammonia (NH₃), and nitrate (NO₃⁻) can be toxic for fish above certain levels (Bergheim and Fivelstad, 2014; Davidson et al., 2017; Mota et al., 2019), and maintaining an acceptable pH level is also crucial. In industrial setups, CO₂ and NH₃ levels are typically monitored indirectly by measuring the concentrations of total inorganic carbon (TIC), total ammonia nitrogen (TAN), and alkalinity. These concentrations remain reaction invariant with respect to pH and the equilibrium reactions that occur during this process, meaning that their concentrations do not change when pH or the concentration of any component involved in the equilibrium reactions fluctuates.

It is possible to develop a dynamic model for these quantities without explicitly including pH in the model by using reaction-invariant quantities, such as TIC, TAN, and alkalinity. Examples of such models can be found in the RAS model developed by Wik et al. (2009) and the model extended by Pedersen and Wik (2020). Both models include fish and bacteria metabolisms, with Pedersen and Wik (2020) extending the model by including a model for the stripper. However, neither model considers the effect of pH explicitly, as it is not necessary when using reaction invariant quantities.

* Corresponding author.

E-mail address: sigurd.skogestad@ntnu.no (S. Skogestad).

To our knowledge, no dynamic models for RAS that consider the effect of pH have been published in the literature. One approach to include pH in the model is to use dynamic balances for all components, including the H^+ concentration, and use the extent of reactions as static coupling variables. However, an alternative approach that uses reaction-invariant variables and fewer differential equations, as proposed for pH systems since the 1980s (Gustafsson and Waller, 1983), may be preferable due to numerical reasons. In this study, we test both approaches and show how the reaction-invariant approach is more suitable.

In this paper, we present simple steady-state and dynamic models that are suitable for controlling and optimizing the design of a RAS (from Nofitech). Our main objective was to develop a water quality model for the main units (fish tank, biofilter, and stripper) that also includes pH, and to study the effects of the placement of substances to adjust pH and alkalinity.

2. Process description

2.1. Process overview

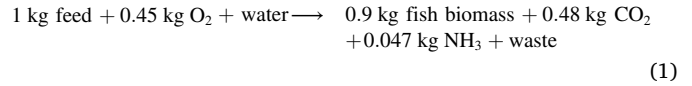
The recirculating aquaculture system is composed of a fish tank and a water treatment system, which includes a biofilter and a CO_2 stripper. Solid removal from the fish tank is also present, but for simplicity, solids are not included in our model. Additionally, denitrifying and disinfection units could be present in other configurations of RAS, but the RAS being studied does not have these types of equipment. An illustration of the process is shown in Fig. 1.

The fish tank receives two inlet streams, one containing fish feed in the form of solid pellets and the other containing recirculated water enriched with oxygen. Fish metabolism takes place in the tank, as described by reaction (1). The effluent water from the fish tank is then sent to the biofilter, where a small amount of makeup water is added. In the biofilter, bacteria convert ammonium into nitrate, as described by reaction (2), with an assumed conversion efficiency of 97% of TAN. The effluent from the biofilter is then sent to a CO_2 stripper, where CO_2 is removed with an efficiency of around 60–70%. To avoid the accumulation of nitrate and other compounds, a purge stream is taken out after the stripper. The remaining recycled water is then fed back to the fish tank after oxygen has been added to an oxygen cone. In Fig. 1, the red lines indicate the four options for pH correction, which can be done in the fish tank (T) and/or in the biofilter (B) by adding base (NaOH) or buffer (NaHCO₃). Although buffer can be used for pH correction, it also adds bicarbonate to the system, making it more difficult to keep low CO_2 levels. Therefore, it is not clear which one should be used. Additionally, we assume that there is a possibility of adding pH correction in the fish

tank, which might not be common practice due to associated risks. However, we assume that the fish farm is knowledgeable about handling this matter and has the power to mitigate it.

2.2. Chemical reactions

In this work, we only focus on modelling the water system of the fish tank and assume that the effect of the fish on the water system can be described by the following empirical chemical equation:



This assumption is based on the premise that the fish receives an adequate amount of feed. In practice, this is determined by monitoring any excess feed and the behavior of the fish. However, there may be instances where the feed is limited for a period, such as when the water is contaminated. In such situations, the biomass growth rate may decrease, and the fish may consume only what is necessary for survival. Nonetheless, in this study, we assume that the fish consumes all the provided feed and that the water quality remains within acceptable limits, thereby not affecting the fish metabolism. In reality, the apparent feed conversion ratio (which is assumed to be 0.9 kg biomass per kg feed) reduces at higher CO_2 concentrations (Khan et al., 2018). However, this effect is not taken into account in this paper. Although the reaction coefficients may vary depending on the fish size, we assume that they are independent for simplicity. That is, we presume that they hold these values during a particular stage in the fish's life cycle while using a standard food type for Atlantic salmon. If the same system is operated throughout a significant part of the fish's life cycle or if the food composition changes, a correction of these coefficients may be necessary.

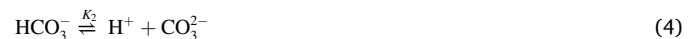
The water treatment system is assumed to be unaffected by fish biomass. Only the consumption of oxygen, as well as the production of carbon dioxide and ammonia, are taken into account as factors that could impact the water treatment process.

The feeding rate in the fish tank typically increases exponentially over a 90-day period as the fish grows from approximately 200 g to 400 g. However, in this paper, we only focus on the first day of operation with a constant fish feed rate of 580.6 g/min.

In the biofilter, nitrifying bacteria convert ammonia to nitrite and then to nitrate, a process known as nitrification (Schreier et al., 2010). In our simulations, we assume that 97% of the TAN (total ammonia nitrogen) is converted, following the overall reaction:



In addition to the biological reactions, it is assumed that all water streams in the process comply with the following acid-base equilibrium reactions:



where K_1 , K_2 , K_3 and K_4 are the equilibrium constants for reactions (3–6). The concentrations of the components in the acid-base reactions depend on pH, which in this paper is computed as

$$pH = -\log_{10}(c_{H^+}/c^0) \quad (7)$$

where $c^0 = 1 \text{ mol/l}$.

In reaction (3), we assume that H_2CO_3 accounts for both H_2CO_3 and

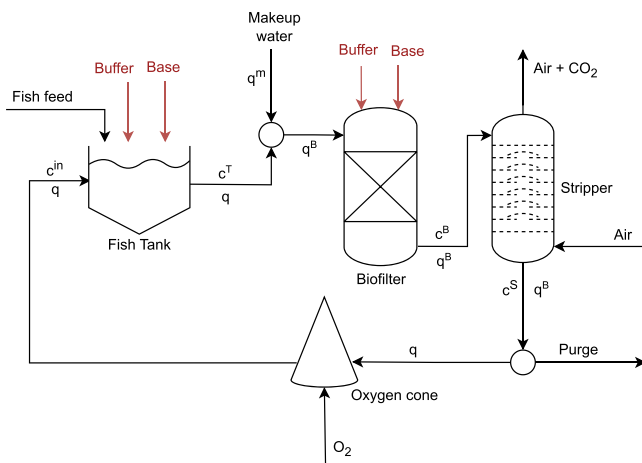


Fig. 1. Flowsheet for RAS process studied in this paper with 4 optional base and buffer intakes (in red lines).

dissolved CO₂, which means that the equilibrium constant, K_1 , also accounts for equilibrium between these two species, represented by the following equilibrium reaction:



Reaction (8) has an equilibrium constant of about $K_0 = 1.2\text{e-}03$ in water, meaning that the concentration of dissolved CO₂ is about 1000 times larger than H₂CO₃. Nevertheless, we represent all dissolved CO₂ and H₂CO₃ as H₂CO₃ in our model.

The model's operational parameters are presented in Table 1, and the physicochemical parameters are listed in Table 2. It is important to note that the equilibrium constants used are not for pure water, but for a mixture of seawater and pure water with a salinity of 15 g/kg and temperature of 14°C. The salinity and temperature have a direct impact on the solubility of the compounds, thereby affecting the equilibrium constants. As a result, there is a shift in the equilibrium graphs compared to fresh water at 25°C (refer to Fig. 2a and b).

Three important variables for the model are TAN, TIC, and alkalinity. These may be viewed as pseudo-components, but, throughout this work, they are included in the components category for simplicity. These pseudo-components are reaction invariants with respect to the equilibrium reactions (3–6), meaning that they are only affected by the in- and outflows of each unit and by the biochemical reactions (1) and (2). The TAN, TIC, and alkalinity concentrations are defined as follows:

$$c_{TAN} = c_{NH_3} + c_{NH_4^+} \quad (9)$$

$$c_{TIC} = c_{H_2CO_3} + c_{HCO_3^-} + c_{CO_3^{2-}} \quad (10)$$

$$c_{alk} = c_{OH^-} + c_{HCO_3^-} + 2c_{CO_3^{2-}} - c_{H^+} + c_{NH_3} \quad (11)$$

It is important to note that these concentrations are typically measured in the laboratory. There are several ways to derive these reaction invariants, and it should be noted that they are not unique since different combinations can be made. One straightforward method is to formulate atom balances for nitrogen, carbon, hydrogen, and oxygen, which involve the eight components that participate in the equilibrium reactions (3–6). TAN can be obtained directly from the nitrogen (N) atom balance, while TIC can be obtained directly from the carbon (C) atom balance. The alkalinity can be derived by stoichiometric considerations (Gustafsson and Waller, 1983) or by combining all four atom balances (H, O, C, N).

Assuming equilibrium in reactions (3–5), Fig. 2a and b illustrate the mole fractions for the carbonate system and ammonia system relative to TIC and TAN as a function of pH, respectively. To maintain low levels of both H₂CO₃ and NH₃ in the fish tank, the pH should be kept within a specific range. From the figures, it is apparent that a pH level above 7 is desirable to achieve low concentrations of H₂CO₃, whereas a pH level below 8 is necessary to achieve low concentrations of NH₃. Thus, a pH range between 7 and 8 is optimal for the fish tank.

The nitrifying bacteria in the biofilter are adaptable to pH, but they do not function well at pH levels below 6 or above 10. The optimal range for their activity is between 7.5 and 8, as reported by Raouliaritiana (2016). Therefore, it is assumed that a satisfactory conversion range falls between 7 and 8. To increase the efficiency of the stripper, it is desirable to have high concentrations of CO₂ (or H₂CO₃ equivalent), as depicted in Fig. 2a. This requires a low pH level to achieve high levels of TIC in the

Table 1
Operational parameters.

Parameter	Value	Unit	Description
ξ^B	0.97	–	Biofilter conversion of TAN
P_{oper}	1	bar	Stripper operating pressure
f_{air}	0.3324	–	Stripper air bypass fraction
V^T	2300	m ³	Tank liquid volume
V^B	282.5	m ³	Biofilter liquid volume

Table 2

Physicochemical parameters at temperature of 14°C, pressure of 1 bar and salinity of 15 g/kg.

Parameter	Value	Unit	Description
K_1	8.9002e-07 ^a	mol/L	Equilibrium constant of reaction (3)
K_2	4.3112e-10 ^a	mol/L	Equilibrium constant of reaction (4)
K_3	9.1592e-10 ^b	mol/L	Equilibrium constant of reaction (5)
K_w	5.2132e-15 ^c	mol ² /L ²	Equilibrium constant of water dissociation
K_H	5.8695e-02 ^d	mol/(L bar)	From Henry's constant for CO ₂ in water
$[O_2]_{sat}$	9.39 ^e	mg/L	O ₂ concentration at 100% saturation
$y_{CO_2}^a$	4.15e-04 ^f	–	CO ₂ mole fraction in air (Sept. 2021)
M_{NH_3}	17.031	g/mol	NH ₃ molar mass
M_{CO_2}	44.010	g/mol	CO ₂ molar mass
M_{NO_3}	62.005	g/mol	NO ₃ molar mass
M_{O_2}	31.998	g/mol	O ₂ molar mass

^aMillero et al. (2006); ^bJohansson and Wedborg (1980); ^cBandura and Lovv (2006), and Millero and Huang (2009); ^dWeiss (1974); ^eBenson and Krause (1984); ^fCalifornia Institute of Technology (2021)

form of H₂CO₃. In practice, it may be better to operate the biofilter at a pH of around 7 to achieve optimal stripper efficiency, although a higher pH level would be better for the bacteria's activity. Alternatively, adding acid between the biofilter and the stripper could resolve this conflict, but this approach is not explored in this study.

3. Process model

3.1. Model assumptions

For simplicity, this section describes all assumptions and the steady-state molar balances, which are then extended to the dynamic model.

The main assumption made for the model is that the system can be described by the chemical reactions (1)–(6). Additionally, several assumptions were made, including:

1. All food is consumed by the fish and the conversion is defined by reaction (1). The biomass increases the mass of the fish, but it is assumed that it does not affect the stoichiometry of reaction (1).
2. The tank and the biofilter are modeled as continuous stirred-tank reactors.
3. Nitrification is assumed to occur only in the biofilter with operating conditions to achieve a given efficiency of TAN conversion according to reaction (2).
4. The stripper is modeled as an equilibrium-stage column with a given air bypass to represent that the real column has less than one equilibrium stage while neglecting the holdup.
5. Neither carbon dioxide nor oxygen is lost to the air in the fish tank or biofilter. Additionally, the variation of the oxygen concentration in the stripper is neglected.
6. The makeup water does not contain TIC, TAN, or alkalinity and does not affect the salinity of the system.
7. Temperature is assumed to be perfectly controlled and not affect fish metabolism.
8. The only relevant addition of water is the makeup water and the only relevant removal is the purge.
9. The levels of the tank and the biofilter are considered perfectly controlled.

These assumptions provide a simplified model for the system, and although they may not capture all the complexities of the real system, they allow for a reasonable estimation of the system's behavior.

The two main approaches for modelling the stripping column are the

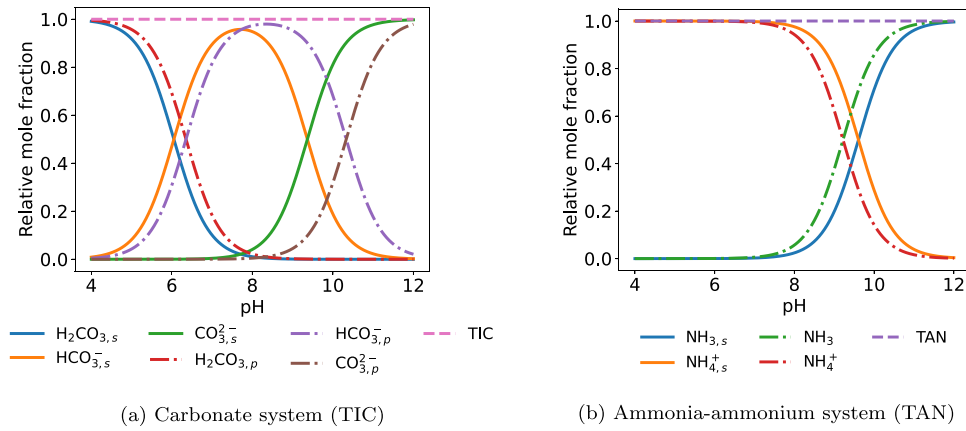


Fig. 2. Relative mole fraction for (a) carbonate system (TIC) and (b) ammonia system (TAN) as a function of pH. Subscript s (solid lines) are values computed for salinity 15 g/kg at temperature 14°C, and subscript p are values computed for pure water at 25°C.

equilibrium-stage model and the two-film mass transfer model. In Vinci et al. (1996), the authors provided a detailed analysis of the latter, which may be more realistic than an equilibrium model. However, this model involves equations with decimal exponents, which can generate imaginary numbers when facing negative arguments during the root-finding process. Therefore, we decided to use an equilibrium-stage model with one stage and a bypass, as in Assumption 4, due to its simplicity and fewer numerical issues. The bypass introduces some non-ideality, which may be realistic since some air volumes may pass through the stripper without reaching equilibrium with the water. Fig. 3 illustrates this modelling approach.

The bypass fraction was determined by comparing the model results with those from an experimental packed column. The column was operated with an inlet CO₂ concentration of 20 mg/L (0.45 mmol/L) and a volumetric gas-to-liquid ratio of 5 and was found to remove 60% of the CO₂ (Summerfelt et al., 2000). Based on this data, the calculated bypass fraction was determined to be 33.24% of the air inlet, as shown in Table 1. It should be noted that as per Assumption 4, the stripper holdup is neglected in the model, resulting in a static stripper model.

3.2. Steady-state molar balances

Based on the aforementioned assumptions, we present below the

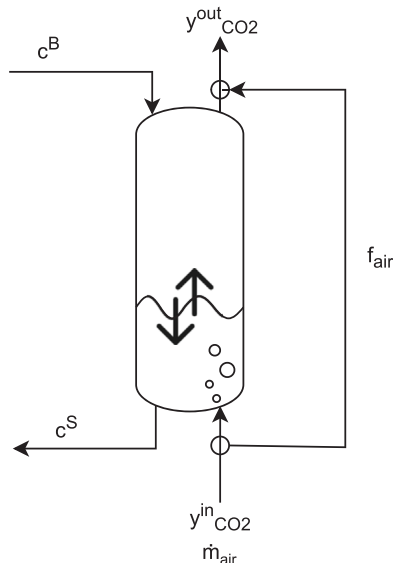


Fig. 3. Simplified model representation of stripper with single equilibrium stage and partial bypass of air.

steady-state molar balances for water, alkalinity, TIC, TAN, nitrate, and oxygen. The variables' names and units are:

- Molar concentration, c [$\text{mol}/\text{m}^3_{\text{water}} = [\text{mmol}/\text{L}_{\text{water}}]$]
- Mass concentration, w [$\text{mg}/\text{L}_{\text{water}}$]
- Liquid flow rate, q [$\text{m}^3_{\text{water}}/\text{min}$]
- Molar flow rate, \dot{m} [mol/min]

3.2.1. Molar balances for water

When considering the mass balance for the mixing point of makeup water, the independent variables or degrees of freedom are the makeup water flow rate, denoted as q^m , and the recirculation flow rate, denoted as q . Based on this, the following equation is obtained:

$$q^B = q + q^m \quad (12)$$

It is assumed that the liquid holdups remain constant at all times. Therefore, the purge flow is equal to the makeup flow (q^m), and the liquid flow rate is q after the purge and before the makeup points. After the makeup and before the purge, the liquid flow rate is q^B , as illustrated in Fig. 1.

3.2.2. Molar balances for alkalinity

- Tank:

$$q c_{alk}^T = q c_{alk}^{in} + \dot{m}_{buffer}^T + \dot{m}_{base}^T + \lambda_{NH_3} F \quad (13)$$

where \dot{m}_{buffer}^T and \dot{m}_{base}^T are the molar flow rates of NaHCO₃ (HCO₃⁻) and NaOH (OH⁻), respectively, being added in the tank. F is the fish feed rate, and λ_{NH_3} is the stoichiometric coefficient for NH₃ in the fish metabolism, given by:

$$\lambda_{NH_3} = \frac{0.047}{M_{NH_3}} \text{ mol} / \text{ g}_{feed}$$

where M_{NH_3} is the molar mass of NH₃.

- Biofilter:

$$q^B c_{alk}^B = q c_{alk}^T + \dot{m}_{buffer}^B + \dot{m}_{base}^B - 2 \zeta^B q c_{TAN}^T \quad (14)$$

where \dot{m}_{buffer}^B and \dot{m}_{base}^B are the molar flow rates [mol/min] of NaHCO₃ and NaOH, respectively, being added in the biofilter. The last term $-2 \zeta^B q c_{TAN}^T$ comes from reaction (2), in which alkalinity has a stoichiometric coefficient of -2 because it forms H⁺ and consumes NH₃.

- Stripper:

$$c_{alk}^S = c_{alk}^B \quad (15)$$

3.2.3. Molar balances for total inorganic carbon (TIC)

- Tank:

$$qc_{TIC}^T = qc_{TIC}^{in} + \dot{m}_{buffer}^T + \lambda_{CO_2} F \quad (16)$$

where \dot{m}_{buffer}^T is the molar flow rate of $NaHCO_3$ being added in the tank, λ_{CO_2} is the stoichiometric coefficient for CO_2 in the fish metabolism, which is given by

$$\lambda_{CO_2} = \frac{0.48}{M_{CO_2}} \text{mol} / g_{feed}$$

- Biofilter:

$$q^B c_{TIC}^B = qc_{TIC}^T + \dot{m}_{buffer}^B \quad (17)$$

where \dot{m}_{buffer}^B is the molar flow rate of $NaHCO_3$ being added in the biofilter.

- Stripper: Assume CO_2 equilibrium between gas and liquid outflow and use the bypass fraction f_{air} to represent that the real stripper has less than one equilibrium stage.

$$q^B c_{TIC}^S + (1 - f_{air}) \dot{m}_{air}^I \frac{y_{CO_2}^{out}}{1 - y_{CO_2}^{out}} = q^B c_{TIC}^B + (1 - f_{air}) \dot{m}_{air}^I \frac{y_{CO_2}^{in}}{1 - y_{CO_2}^{in}} \quad (18)$$

$$y_{CO_2}^{out} = \frac{c_{H_2CO_3}^S}{K_H P_{oper}} \quad (19)$$

where \dot{m}_{air}^I is the molar flow rate of air excluding its CO_2 content, and $y_{CO_2}^{out}$ is the molar fraction of CO_2 at the outlet stream, meaning that the total air flow rate at the inlet stream is given by $\dot{m}_{air} = \frac{\dot{m}_{air}^I}{1 - y_{CO_2}^{out}}$.

3.2.4. Molar balances for total ammonia nitrogen (TAN)

- Tank:

$$qc_{TAN}^T = qc_{TAN}^{in} + \lambda_{NH_3} F \quad (20)$$

- Biofilter:

$$q^B c_{TAN}^B = qc_{TAN}^T - \xi^B qc_{TAN}^T \quad (21)$$

- Stripper:

$$c_{TAN}^S = c_{TAN}^B \quad (22)$$

3.2.5. Molar balances for nitrate

The NO_3^- ions are only produced in the biofilter and removed by the purge, so we have at steady state:

- Tank:

$$c_{NO_3^-}^T = c_{NO_3^-}^{in} \quad (23)$$

- Biofilter:

$$q^B c_{NO_3^-}^B = qc_{NO_3^-}^T + \xi^B qc_{TAN}^T \quad (24)$$

- Stripper:

$$c_{NO_3^-}^S = c_{NO_3^-}^B \quad (25)$$

3.2.6. Molar balances for oxygen

- Tank:

$$qc_{O_2}^T = qc_{O_2}^{in} - \lambda_{O_2} F \quad (26)$$

where λ_{O_2} is the stoichiometric coefficient of O_2 in the fish metabolism, which is given by

$$\lambda_{O_2} = \frac{0.45}{M_{O_2}} \text{mol} / g_{feed}$$

- Biofilter:

$$q^B c_{O_2}^B = qc_{O_2}^T - 2\xi^B qc_{TAN}^T \quad (27)$$

- Stripper:

$$c_{O_2}^S = c_{O_2}^B \quad (28)$$

- Purge + Oxygen cone:

$$qc_{O_2}^{in} = qc_{O_2}^S + \dot{m}_{O_2} \quad (29)$$

where \dot{m}_{O_2} is the molar flow rate of oxygen being injected into the stream in the oxygen cone.

Note that, except for O_2 , which is added between the biofilter and the tank, we have that $c^{in} = c^S$.

The pH values at the different locations are calculated based on the provided concentrations of alkalinity, TIC, and TAN using Eq. (30), as explained next. The concentrations of ionic species can be determined from the calculated pH values using the equilibrium reactions (3–6).

3.3. Computation of pH

In addition to the molar balances of reaction invariants, the acid-base equilibrium in the system must also be considered in order to compute the pH, along with the concentration of the species in equilibrium. This was done by writing the equilibrium relations between species, according to reactions (3–6), and solving the resulting system of algebraic equations as a function of the reaction invariants.

A simple analytic expression for alkalinity was developed by Henson and Seborg (1994), which enables the calculation of c_{H^+} as a function of c_{TIC} and c_{alk} . We extend this analysis by including the dependence on c_{TAN} to incorporate the ammonia-ammonium equilibrium. The resulting analytic expression, which is used to compute c_{H^+} (or pH) at each unit (fish tank, biofilter, and stripper), becomes:

$$c_{alk}^i = c_{TIC}^i \frac{K_1 c_{H^+}^i + 2K_1 K_2}{(c_{H^+}^i)^2 + K_1 c_{H^+}^i + K_1 K_2} + \frac{K_w}{c_{H^+}^i} - c_{H^+}^i + c_{TAN}^i \frac{K_3}{c_{H^+}^i + K_3}, \quad (30)$$

$$i = T, B, S$$

In the Appendix, we show in detail how this expression was derived and its extension to include the equilibrium of phosphate ions, if these are present.

3.4. Dynamic molar balances

This section describes the generalized model which can be utilized for simulating steady-state and dynamic behavior. The model equations are consistent with the previous sections but presented in a more general form. The model considers five species or components, namely alkalinity, TIC, TAN, NO_3^- , and O_2 . The molar balances for these five components in the tank and the biofilter are described by Eq. (31) and (32), respectively.

$$V^T \frac{dc^T}{dt} = q(c^{in} - c^T) + g^T + h^T \quad (31)$$

$$V^B \frac{dc^B}{dt} = q^B \left(c^T \frac{q}{q^B} - c^B \right) + g^B + h^B \quad (32)$$

where c^{in} , c^T , c^B and c^S are column vectors containing the concentration of the five species at the inlet of the tank, in the fish tank, in the biofilter, and in the stripper, respectively. g^T and g^B are column vectors representing the amount of each component coming from input streams to the tank and biofilter, respectively, and h^T and h^B are column vectors containing the amount of each component generated or removed in the reactions (1) and (2), respectively. From this, g^T , g^B , h^T and h^B are defined as follows:

$$g^T = \begin{bmatrix} \dot{m}_{buffer}^T + \dot{m}_{base}^T \\ \dot{m}_{buffer}^T \\ 0 \\ 0 \\ 0 \end{bmatrix} \quad g^B = \begin{bmatrix} \dot{m}_{buffer}^B + \dot{m}_{base}^B \\ \dot{m}_{buffer}^B \\ 0 \\ 0 \\ 0 \end{bmatrix}$$

$$h^T = \begin{bmatrix} \lambda_{NH_3} F \\ \lambda_{CO_2} F \\ \lambda_{NH_3} F \\ 0 \\ -\lambda_{O_2} F \end{bmatrix} \quad h^B = \begin{bmatrix} -2q\zeta^B c_{TAN}^T \\ 0 \\ -q\zeta^B c_{TAN}^T \\ q\zeta^B c_{TAN}^T \\ -2q\zeta^B c_{TAN}^T \end{bmatrix}$$

The set of ordinary differential equations (ODEs) presented above comprises a total of 10 equations, which govern the dynamics of the system. In addition, there are 4 static equations that describe the molar balances in the stripper and oxygen cone.

To implement this system, we use a set of 10 differential states, as given in Eqs. (31) and (32), which are derived from the molar balances of TIC, TAN, alkalinity, oxygen, and nitrate in the tank and biofilter. We also use 4 algebraic states, as given in Eqs. (18) and (30), which calculate the values of c_{TIC}^S and c_{H^+} after passing through the three units (tank, biofilter, and stripper). Although c_{H^+} (pH) is not necessary for dynamic simulation of the tank and biofilter, unless one wants to know the pH and individual species concentrations, it is required for modelling the stripper, as the H_2CO_3 concentration is the driving force for TIC removal.

4. Degrees of freedom for operation

The system can be operated through several manipulated variables (i.e., dynamic degrees of freedom), as illustrated in Fig. 4. These variables are:

1. Fish feed (pellets);
2. Recirculation flow (i.e., liquid inflow to tank);
3. Liquid outflow from the tank;
4. Liquid inflow to biofilter;
5. Liquid outflow from biofilter;

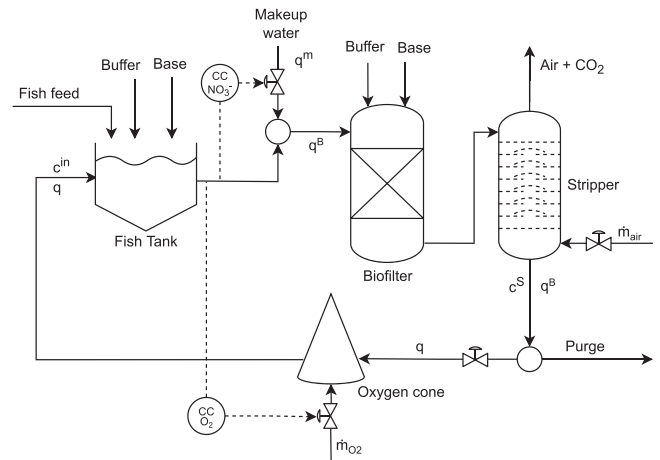


Fig. 4. Flowsheet of RAS process where the valve symbols show control degrees of freedom. Two stabilizing controllers for nitrate and oxygen are included. In addition, we usually have a stabilizing pH controller using buffer/base addition.

6. Liquid outflow from stripper;
7. Liquid inflow to oxygen unit;
8. Pure oxygen feed;
9. Heating/cooling;
10. Purge;
11. Makeup water;
12. Air inflow to stripper;
13. Base/buffer added to tank/biofilter

The last variable could potentially represent up to four degrees of freedom, although typically only one is used at a time. When proposing the model, it was assumed constant liquid holdup in the fish tank, biofilter, stripper, oxygen unit, mixing point for makeup water, and exit point for purge. This enabled us to establish six molar balances, which we could utilize to eliminate six of the previously mentioned variables. For instance, by taking into account the total holdup in all units, we determined that the purge flow was equal to the makeup water flow rate, q^m . Additionally, the feed to the biofilter was equivalent to the sum of the liquid flow out of the fish tank and the makeup water. Furthermore, the liquid flow rate of the outlet of the fish tank, biofilter, stripper, and oxygen unit was equivalent to their respective inlet flow rates. To simplify the system further, we assumed that the temperature of the liquid streams was perfectly controlled, removing the heating/cooling as a degree of freedom. In total, this eliminates seven degrees of freedom, leaving us with six steady-state degrees of freedom for operation and control. For our simulations, we consider the fish feed, F , as a measured disturbance. As a result, we focus on the five degrees of freedom (manipulated variables) for operation, which are provided in Table 3.

The process flowsheet is shown in Fig. 4, with the first four degrees of freedom indicated with valve symbols. The degree(s) of freedom related to buffer/base addition is not assigned in this flowsheet, as it can be any of the buffer/base feed streams. Moreover, the flowsheet includes two stabilizing controllers to control the nitrate and oxygen concentrations in the tank, which are later used in the dynamic simulations.

Table 3

Control degrees of freedom (manipulated variables) with steady-state effect.

Description	Variable	Unit
Recirculation flow rate	q	m^3/min
Air feed to stripper	\dot{m}_{air}	mol/min
Oxygen feed	\dot{m}_{O_2}	mol/min
Makeup water	q^m	m^3/min
Base/buffer feed	$\dot{m}_{base}/\dot{m}_{buffer}$	mol/min

Table 4
Nominal operational specifications used in simulations.

Variable	Value	Unit	Description
q	30	m ³ /min	Recirculation flow rate
\dot{m}_{air}	6285	mol/min	Air feed to stripper
$c_{O_2\%}$	80%	–	O ₂ saturation
$w_{NO_3^-}^T$	100	mg/L	NO ₃ ⁻ mass concentration in fish tank
pH^B	7.05	–	pH in biofilter
F	580.6	g/min	Fish feed rate on day 1

Table 5
Required addition of **base** (NaOH) or **buffer** (NaHCO₃) to keep desired pH in biofilter in each scenario [mol/min].

Variable	Scenario 1	Scenario 2	Scenario 3	Scenario 4
\dot{m}_{base}^T	3.75	0	0	0
\dot{m}_{base}^B	0	3.75	0	0
\dot{m}_{buffer}^T	0	0	5.46	0
\dot{m}_{buffer}^B	0	0	0	5.46

Table 6
Steady-state concentrations [mmol/L or -] for each unit for Scenario 1.

Variables	Tank	Biofilter	Stripper
c_{alk}	2.2458	2.0706	2.0706
c_{TIC}	2.341	2.2661	2.13
$c_{H_2CO_3}$	0.1159	0.2054	0.0833
c_{TAN}	0.055	0.0016	0.0016
c_{NH_3}	2.8901e-04	4.4167e-06	1.0700e-05
$c_{NO_3^-}$	1.6128	1.6128	1.6128
c_{O_2}	0.2348	0.124	0.124
pH	7.3299	7.05	7.436

With a given feed rate, there are five steady-state operational degrees of freedom, and therefore we need five specifications to define the operation. In the simulations, we use a typical set of specifications provided in Table 4. Out of these specifications, two are on manipulated variables (MVs), namely the recirculation flow rate and air feed to the stripper, while the other three are on controlled variables (CVs). These three CV specifications (O₂ saturation, nitrate concentration, and pH) indirectly determine the value of the three remaining MVs (O₂ feed, makeup water, base/buffer addition).

5. Simulation results

In this section, we present some steady-state and dynamic simulation results, which also contribute to validating the model.

5.1. Steady-state simulations

For the steady-state calculations, we utilized the five specifications in Table 4 in combination with the given feed rate. It is worth noting that we maintained the oxygen level, the nitrate level, and the pH in the biofilter at fixed values. To achieve control of the pH in the biofilter, we considered four different scenarios, where we implemented one type of pH/alkalinity adjustment at a time (see Fig. 4):

- 1) Base addition in the tank (\dot{m}_{base}^T)
- 2) Base addition in the biofilter (\dot{m}_{base}^B)
- 3) Buffer addition in the tank (\dot{m}_{buffer}^T)
- 4) Buffer addition in the biofilter (\dot{m}_{buffer}^B)

The steady-state system was solved for the four scenarios considering the conditions for day 1. The makeup water flow rate was the same in all scenarios ($q^m = 0.992 \text{ m}^3/\text{min}$) because the nitrate concentration was

Table 7
Steady-state concentrations [mmol/L or -] for each unit for Scenario 2.

Variables	Tank	Biofilter	Stripper
c_{alk}	2.124	2.0706	2.0706
c_{TIC}	2.341	2.2661	2.13
$c_{H_2CO_3}$	0.2266	0.2054	0.0833
c_{TAN}	0.055	0.0016	0.0016
c_{NH_3}	1.4151e-04	4.4167e-06	1.0700e-05
$c_{NO_3^-}$	1.6128	1.6128	1.6128
c_{O_2}	0.2348	0.124	0.124
pH	7.0186	7.05	7.436

Table 8
Steady-state concentrations [mmol/L or -] for each unit for Scenario 3.

Variables	Tank	Biofilter	Stripper
c_{alk}	3.846	3.6195	3.6195
c_{TIC}	4.0922	3.9612	3.7081
$c_{H_2CO_3}$	0.2721	0.359	0.1338
c_{TAN}	0.055	0.0016	0.0016
c_{NH_3}	2.1214e-04	4.4167e-06	1.1611e-05
$c_{NO_3^-}$	1.6128	1.6128	1.6128
c_{O_2}	0.2348	0.124	0.124
pH	7.195	7.05	7.4717

Table 9
Steady-state concentrations [mmol/L or -] for each unit for Scenario 4.

Variables	Tank	Biofilter	Stripper
c_{alk}	3.6729	3.6195	3.6195
c_{TIC}	3.9192	3.9612	3.7081
$c_{H_2CO_3}$	0.2701	0.359	0.1338
c_{TAN}	0.055	0.0016	0.0016
c_{NH_3}	2.0427e-04	4.4167e-06	1.1611e-05
$c_{NO_3^-}$	1.6128	1.6128	1.6128
c_{O_2}	0.2348	0.124	0.124
pH	7.1785	7.05	7.4717

specified. Since the recirculation flow rate, q , was specified at 30 m³/min, the recirculation ratio was $r = q/(q + q^m) = 0.968$ in all scenarios. The oxygen feed rate was constant for all scenarios at 11.49 mol/min. The results presented in Table 5 indicate that the amount of base or buffer is the same regardless of the location where it is added.

Tables 6, 7, 8, 9 present the results obtained from the steady-state simulation. We see that the pH in the fish tank was generally higher than in the biofilter in most scenarios, except in Scenario 2 where base was added to the biofilter. The decrease in TAN and oxygen concentrations from the tank to the biofilter can be attributed to reaction (2) and dilution by the makeup water. In terms of maximizing fish growth, low levels of NH₃ and CO₂ (H₂CO₃) are preferred in the fish tank. The pH in the fish tank significantly affects these values. For instance, a high pH of 7.34 resulted in a high concentration of ammonia (Scenario 1), while a low pH of 7.01 resulted in a high concentration of H₂CO₃ (Scenario 2). To achieve low levels of CO₂, it is better to use NaOH (base) (Scenarios 1 and 2) instead of NaHCO₃ (buffer) for pH adjustment.

Despite using a large amount of buffer, Scenarios 3 and 4, which both use sodium bicarbonate (buffer) for pH adjustment, have almost identical steady-state values. This result is expected due to the well-known buffer effect.

5.2. Dynamic simulation

Figure Fig. 5 illustrates the dynamic response of the system to a step increase of 56.5 g/min in the fish feed (about 10% disturbance) with all the five manipulated variables kept constant, including the oxygen

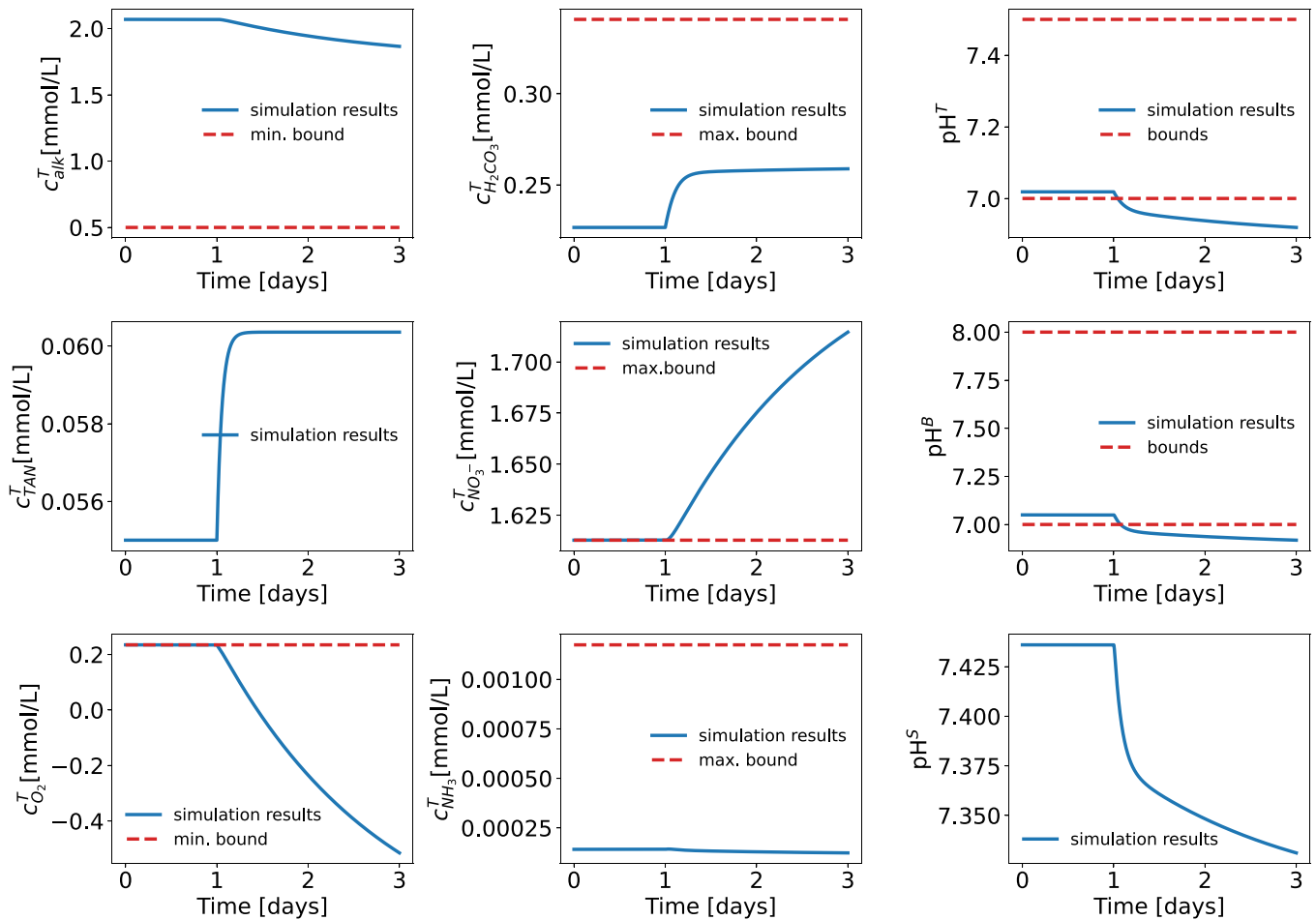


Fig. 5. Dynamic behavior for a step change of 56.5 g/min in the fish feed, F , at day 1, with no oxygen and nitrate control.

addition.

The simulation results indicated that the fish would not survive, even for a day, mainly due to the oxygen level becoming negative in less than one day. This result was caused by the consumption of oxygen according to reaction (1). Furthermore, the nitrate concentration steadily increased, which is harmful to the fish.

To prevent negative oxygen levels and the buildup of nitrate in the system, the oxygen intake was controlled in the fish tank, and makeup water addition was used to control nitrate in the tank, as shown in Fig. 4.

With those controllers, we see in Fig. 6 that oxygen and nitrate concentrations are now kept constant, but other variables still go out of bounds, including the pH in the tank and in the biofilter. This indicates the need to introduce additional control loops, using buffer or base addition. However, since the aim of this work was to present the process modeling, a more detailed control design will be considered in future work.

6. Comparison with real data

To validate the model, we compared it to data collected from a commercial fish farm of Atlantic salmon that used the same RAS configuration as in Scenario 2, where base was added to the biofilter to regulate the pH. The data was collected over a 44-day period and consisted of sensor readings taken every 30 min, including temperature (T), salinity (S), oxygen saturation ($c_{O_2\%}$), and pH in the fish tank (pH^T) and stripper (pH^S), as well as various flow rates. Laboratory measurements were also taken every other day on the outflow from the tank, which included the concentrations of NO_3^- , H_2CO_3 , TAN, and alkalinity (c_{alk}^*). Fig. 7 displays the average daily measurements of temperature and

salinity.

In Fig. 8, we compare the measured data with the simulated dynamic responses. The upper six plots display the six operational degrees of freedom, including the fish feed. The lower nine plots show six concentrations in the fish tank (T) along with the pH after the fish tank, biofilter, and stripper.

The simulation model is similar to the one described earlier, with the exception of the stoichiometric coefficient for ammonia in reaction (1), which was halved to 0.0235 to better match the experimental data for TAN concentration in the fish tank. The variation in the stoichiometric coefficients is expected as they depend on the composition of the fish feed. Since the measured temperature and salinity are not constant, the equilibrium constants change slightly over time as they are a function of temperature and salinity.

It is important to note that the simulated responses were not generated by directly entering the independent variables, i.e., feed flow rates, into the dynamic model. This is because some flow rates were missing from the data, such as air and oxygen inlet streams, and directly entering the measured base flow rate would have resulted in significant offsets in pH and other concentrations. This is due to the model predictions being highly sensitive to errors in the base feed flow rate. Instead, the pH and concentration measurements were used as setpoints, since these are more reliable, and feedback controllers were employed to adjust the feed flow rates and match them with the measured values.

In order to match the simulation results with the measured data, several adjustments were made to the model inputs. The details of these adjustments are outlined below:

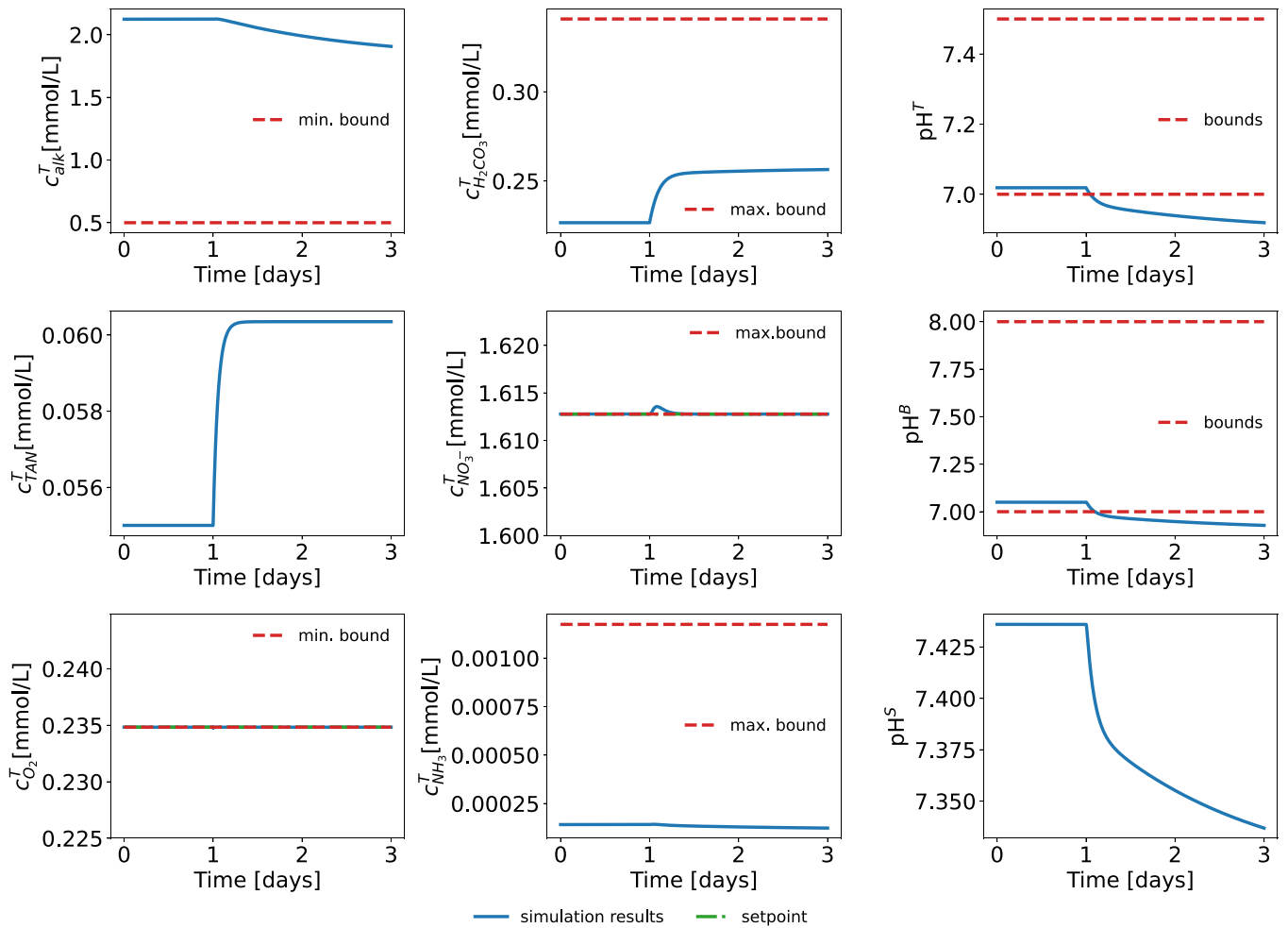


Fig. 6. Dynamic behavior for a step change of 56.5 g/min in the fish feed, F , at day 1, with oxygen and nitrate controllers.

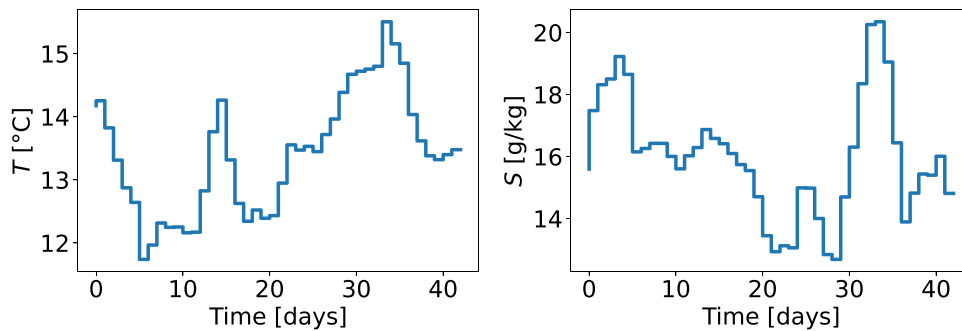


Fig. 7. Temperature and salinity measured data.

- The measured data for fish feed, denoted as F , was used in the model after excluding the very small values. To account for situations where the fish stop eating and operators stop feeding (which leads to these excluded values), the feed rate was always set to be higher than a minimum amount of $50\%F^i$, where F^i is the planned amount of feed for day i . Moreover, due to the nature of the data, which reports the cumulative mass of food each day, we assumed a step-like feed rate for each day, which may result in occasional large deviations in concentrations.
- The measured rate of makeup water, q^m , was used directly in the model.
- The measured recirculation rate, q , was also used directly in the model. It remained almost constant over the 44-day period, except for two days with slightly lower values.
- The airflow to the stripper, \dot{V}_{air} , was not measured, so it was assumed to be 10 times the recirculation flow rate of project, which was assumed to be $23.7 \text{ m}^3/\text{min}$ (the mean of all q).
- The flow rate of the oxygen inlet was not measured. It was estimated by matching the measured and simulated oxygen concentrations using a feedback O_2 controller with the measured oxygen saturation as the setpoint.
- The base addition was calculated by matching the measured and simulated pH after the stripper, using a feedback pH controller with

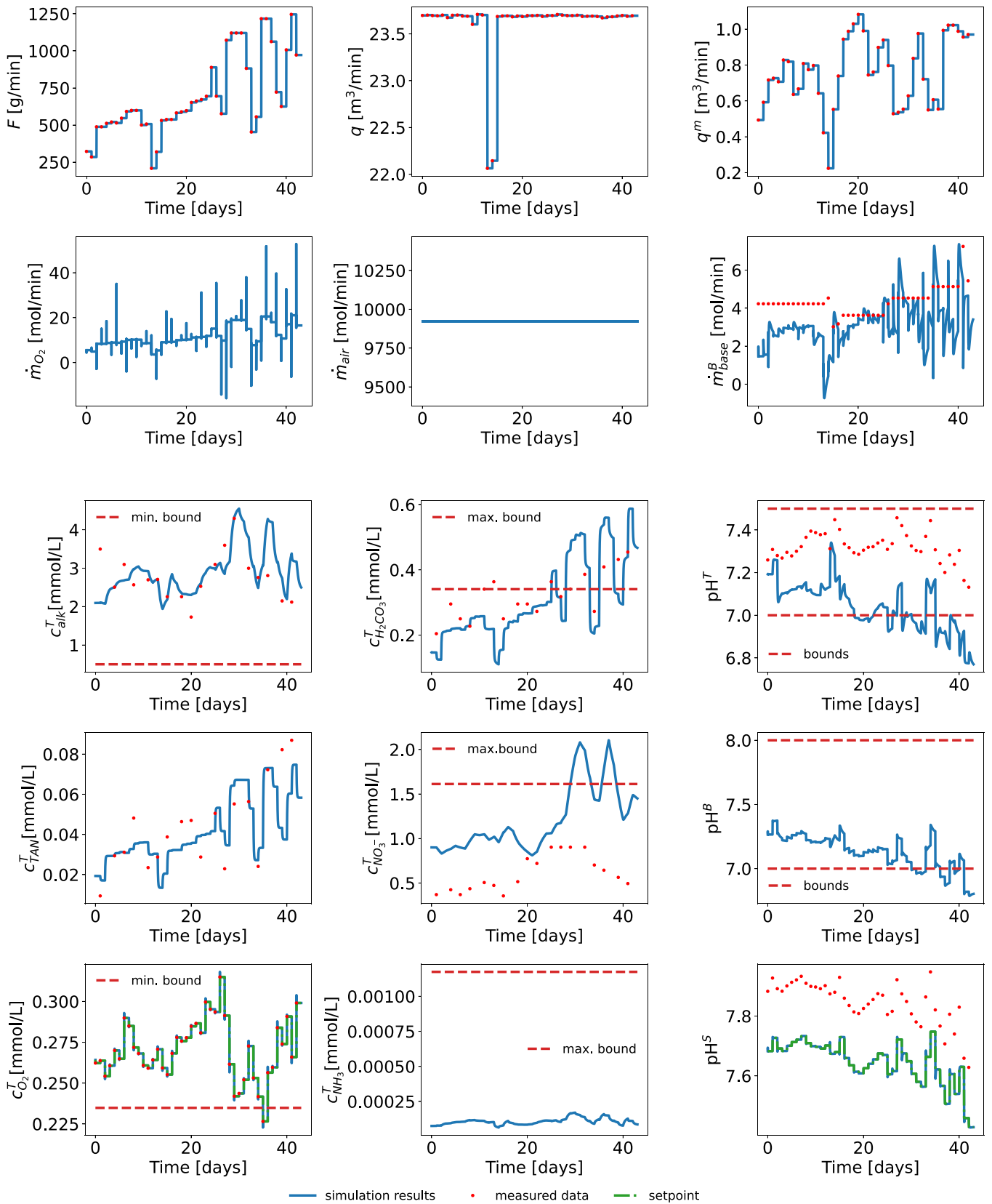


Fig. 8. Simulated (blue lines) and measured (red dots) flow rates and concentrations for a real RAS plant over a 44-day period.

the daily average of measured pH as the setpoint. To improve the match with other measured data, such as alkalinity and $\text{CO}_2/\text{H}_2\text{CO}_3$ concentrations in the fish tank, a bias of 0.2 pH units was introduced for the measured pH after the stripper. This means that the simulated pH after the stripper is 0.2 units lower than the measured value (see the lower right plot in Fig. 8).

The calculated base addition showed significant deviations from the measured value, particularly during the first 14 days, which could be attributed to measurement errors. The later deviations or peaks could be explained by inaccuracies in the feed rate F , leading to errors in the CO_2 produced by fish metabolism, and thereby affecting the pH and the amount of base required. The bias of 0.2 pH units introduced in the stripper was carried over to the fish tank, resulting in a similar deviation. The reason for the deviation could be a sensor error or modelling inaccuracies in the thermodynamics, which were not modelled in much detail. The simulated concentrations of TAN, alkalinity, and H_2CO_3 in the fish tank were in good agreement with the measured values from the laboratory. The simulated pH was also close to the measured values, except for the bias of about 0.2 pH units. In Assumption 3, the constant conversion of TAN might not always reflect reality. The operating region under study includes a change in behavior of the conversion of TAN, where a constant value provides a better representation of reality (0.1–0.5 $\text{mg}_{\text{TAN}}/\text{L}$), and beyond which the Monod model might be more suitable (when TAN mass concentration exceeds 0.5 mg/L) (Malone et al., 2006). To evaluate the impact of TAN conversion on concentrations, a sensitivity analysis was conducted, revealing that it only had a significant effect on TAN concentration. This can be attributed to the disparity in magnitudes between nitrate and ammonia quantities, resulting in the efficiency effect being negligible on nitrate concentration. Consequently, the nitrate concentration is primarily influenced by purge/makeup water. Fig. 9 illustrates that the amount of nitrate formation in the biofilter is insufficient to significantly impact its concentration.

The simulated nitrate concentration was approximately twice the measured value, which could be attributed to the accumulation of nitrate in the recirculating system due to the small purge. In the model, some of the nitrogen from the feed exits the system in the purge, mainly as nitrate. Since the simulated TAN concentration in the fish tank was similar to the measured values, it is likely that the actual system has other nitrate exits, such as in solid waste and denitrification in the biofilm. However, the model did not account for solids or denitrification. Therefore, the fish farm system could benefit from nitrate control to better use of the makeup water.

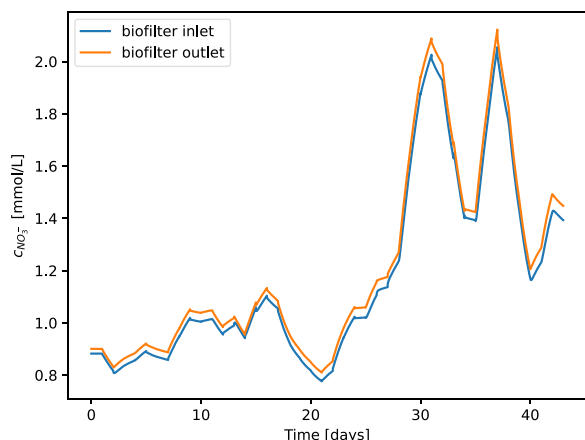


Fig. 9. Nitrate concentrations before and after the nitrification in the biofilter.

7. Discussion

7.1. Stripper model

At first, we attempted to model the stripper by assuming a constant efficiency. However, this resulted in the existence of multiple solutions, each of them in a different pH zone. Therefore, it was numerically better and more physically correct to model the stripping unit as a single-stage equilibrium column with some air bypass. In this model, the efficiency was indirectly dependent on the pH, as the concentration of H_2CO_3 available for stripping depends on pH.

7.2. Numerical solver

CasADi is an open-source tool that enables nonlinear optimization and algorithmic differentiation. Its symbolic framework facilitates model simulation and implementation of numerical optimal control, which is the intended focus of future work. The equation systems were solved using CasADi version 3.5.5 in Python version 3.8.8, and required a DAE solver, so IDAS from Suite of Nonlinear and Differential/ALgebraic Equation Solvers (SUNDIALS) (Hindmarsh et al., 2005), distributed along with CasADi, was used for the steady-state and dynamic simulations.

7.3. Use of reaction invariants

In this work, the model development relied on incorporating three reaction invariants, namely TAN, TIC, and alkalinity. Instead of representing individual components, including pH, as dynamic states, static equilibrium relationships like Eq. (30) were used to obtain their concentrations.

An alternative, and more straightforward, approach for this modeling involves writing dynamic balances for all chemical components and introducing four extents of reactions to represent reactions (3)–(6). This model was also implemented, and the results agree with the model presented in this work, which serves as validation of the proposed model. While the model based on the extent of reactions avoids the use of reaction invariants, which can be non-physical quantities, it resulted in numerical difficulties. The steady-state solution was highly dependent on the initial condition, often leading to infeasibility with negative concentrations. To overcome this issue, a numerical trick was used by making these states equal to the exponential of the concentrations. While this solved the infeasibility problem, the numerical solver could still diverge with the iterations approaching very high concentrations. Thus, the approach based on reaction invariants was preferred as it was more stable and reliable.

7.4. Steady-state simulations

The steady-state simulation yielded valuable insights into the system. Because of the nitrate requirement, the amount of makeup water was constant in all scenarios. To decrease the amount the makeup water, one may add a denitrification unit to the process to convert nitrate into nitrogen gas, as suggested by Tal et al. (2009).

The steady-state results presented in Tables 6–9 indicate that the concentration of H_2CO_3 in the tank was the lowest in Scenario 1 ($c_{\text{H}_2\text{CO}_3}^T = 0.1257 \text{ mmol}/\text{L}$), where base was added in the biofilter, which is preferable for fish growth since they thrive best with low H_2CO_3 levels (Khan et al., 2018). On the other hand, the pH in the tank was also the highest in Scenario 1 ($\text{pH}^T = 7.3142$), resulting in a high concentration of ammonia ($c_{\text{NH}_3}^T = 2.755 \text{ e-}04 \text{ mmol}/\text{L}$). Previous research has shown that high H_2CO_3 levels have a negative impact on fish growth, while high ammonia concentrations induce stress, which also affects growth (Thorarensen and Farrell, 2011).

8. Conclusion

A generalized and simplified steady-state and dynamic model of a Recirculating Aquaculture System (RAS) water treatment was developed for control and optimization purposes.

Dynamic simulation of a nominal case with no control (Fig. 5) revealed the importance of a basic stabilization control structure that included controlling the oxygen and nitrate concentrations in the fish tank (Fig. 6). Additionally, pH needs to be controlled in practice, and steady-state results in Tables 6–9 show four scenarios using base or buffer to control the pH in the biofilter. The optimal location of the base or buffer feed and the choice between the two require detailed analysis, as it depends on economic factors.

The proposed model demonstrated excellent performance when simulated using real data, resulting in a trajectory with high similarity to reality, considering the simplified nature of the model. However, to obtain more accurate carbon dioxide and nitrate levels, all losses of these quantities should be taken into account.

Overall, the proposed model is numerically robust and well-suited for further studies on optimal operation and control of RAS water treatment systems.

CRedit authorship contribution statement

Allyne M. dos Santos: Conceptualization, Methodology, Software,

Appendix A. Derivation of Eq. (30)

Eq. (30) is used to compute pH as a function of the concentrations of the reaction invariants (TAN, TIC, and alkalinity). Comparing Eq. (30) with the equivalent equation in Henson and Seborg (1994), an extra term for TAN is added, which is caused by the contribution of NH_3 in the alkalinity definition.

Recall from Eq. (11) that the alkalinity is defined as:

$$c_{alk} = c_{OH^-} + c_{HCO_3^-} + 2c_{CO_3^{2-}} - c_{H^+} + c_{NH_3} \quad (\text{A.1})$$

To derive Eq. (30), we need expressions for each species concentration as a function of c_{H^+} and the reaction invariants. First, we have that $c_{OH^-} = K_w/c_{H^+}$.

For the carbonate system, the equilibrium reactions and the definition of TIC concentration give:

$$c_{HCO_3^-} = K_1 \frac{c_{H_2CO_3}}{c_{H^+}} \quad (\text{A.2})$$

$$c_{CO_3^{2-}} = K_2 \frac{c_{HCO_3^-}}{c_{H^+}} = K_1 K_2 \frac{c_{H_2CO_3}}{(c_{H^+})^2} \quad (\text{A.3})$$

$$c_{TIC} = c_{H_2CO_3} + c_{HCO_3^-} + c_{CO_3^{2-}} \quad (\text{A.4})$$

Combining Eqs. (A.2)–(A.4) gives:

$$c_{H_2CO_3} = c_{TIC} \left(1 + \frac{K_1}{c_{H^+}} + \frac{K_1 K_2}{(c_{H^+})^2} \right)^{-1} \quad (\text{A.5})$$

$$c_{HCO_3^-} = c_{TIC} \frac{K_1}{c_{H^+}} \left(1 + \frac{K_1}{c_{H^+}} + \frac{K_1 K_2}{(c_{H^+})^2} \right)^{-1} \quad (\text{A.6})$$

$$c_{CO_3^{2-}} = c_{TIC} \frac{K_1 K_2}{(c_{H^+})^2} \left(1 + \frac{K_1}{c_{H^+}} + \frac{K_1 K_2}{(c_{H^+})^2} \right)^{-1} \quad (\text{A.7})$$

For ammonium, the ammonia-ammonium equilibrium reaction and the definition of TAN concentration give:

$$c_{NH_3} = K_3 \frac{c_{NH_4^+}}{c_{H^+}} \quad (\text{A.8})$$

$$c_{TAN} = c_{NH_3} + c_{NH_4^+} \quad (\text{A.9})$$

Combining Eqs. (A.8) and (A.9) gives:

Validation, Formal analysis, Investigation, Data Curation, Writing - Original Draft, Writing - Review & Editing, Visualization. **Lucas F. Bernardino:** Methodology, Software, Validation, Writing - Review & Editing. **Kari J.K. Attramadal:** Conceptualization, Validation, Investigation, Data Curation, Writing - Review & Editing, Supervision. **Sigurd Skogestad:** Conceptualization, Methodology, Validation, Investigation, Writing - Review & Editing, Supervision.

Declaration of Competing Interest

The authors declare that they have no known competing financial interests or personal relationships that could have appeared to influence the work reported in this paper.

Data availability

The data that has been used is confidential.

Acknowledgements

The authors acknowledge the commercial fish farm for disclosing the data for this work to be more complete. We also thank Andrea Tuveri for the useful comments on this paper.

$$c_{NH_3} = K_3 \frac{c_{TAN}}{c_{H^+}} \left(1 + \frac{K_3}{c_{H^+}}\right)^{-1} = c_{TAN} \frac{K_3}{c_{H^+} + K_3} \quad (A.10)$$

Substituting these expressions into the definition of alkalinity in Eq. (A.1) gives:

$$c_{alk} = \frac{K_w}{c_{H^+}} + c_{TIC} \frac{K_1}{c_{H^+}} \left(1 + \frac{K_1}{c_{H^+}} + \frac{K_1 K_2}{(c_{H^+})^2}\right)^{-1} \left(\frac{K_1}{c_{H^+}} + 2 \frac{K_1 K_2}{(c_{H^+})^2}\right) - c_{H^+} + c_{TAN} \frac{K_3}{c_{H^+} + K_3} \quad (A.11)$$

or

$$c_{alk} = c_{TIC} \frac{K_1 c_{H^+} + 2K_1 K_2}{(c_{H^+})^2 + K_1 c_{H^+} + K_1 K_2} + \frac{K_w}{c_{H^+}} - c_{H^+} + c_{TAN} \frac{K_3}{c_{H^+} + K_3} \quad (A.12)$$

which is the desired expression (30).

Phosphate. The expression in (A.12) may be extended to include other acids or bases. Specifically, if we include phosphate in the system, which is common in wastewater treatment systems, a fourth reaction invariant is needed, namely total phosphorus (TP):

$$c_{TP} = c_{H_3PO_4} + c_{H_2PO_4^-} + c_{HPO_4^{2-}} + c_{PO_4^{3-}} \quad (A.13)$$

Additional terms must be added to the alkalinity definition to account for $H_2PO_4^-$, HPO_4^{2-} , and PO_4^{3-} contributions. From atomic balances, the alkalinity with phosphate included becomes:

$$c_{alk} = c_{OH^-} + c_{HCO_3^-} + 2c_{CO_3^{2-}} - c_{H^+} + c_{NH_3} + c_{H_2PO_4^-} + 2c_{HPO_4^{2-}} + 3c_{PO_4^{3-}} \quad (A.14)$$

For the phosphate system, we have, from its three equilibrium reactions:

$$c_{H_2PO_4^-} = K_4 \frac{c_{H_3PO_4}}{c_{H^+}} \quad (A.15)$$

$$c_{HPO_4^{2-}} = K_5 \frac{c_{H_2PO_4^-}}{c_{H^+}} \quad (A.16)$$

$$c_{PO_4^{3-}} = K_6 \frac{c_{HPO_4^{2-}}}{c_{H^+}} \quad (A.17)$$

Combining the definition of TP in Eq. (A.13) with Eqs. (A.15)–(A.17) gives the following expression for the three contributions from phosphate to alkalinity (c_{alk}):

$$c_{H_2PO_4^-} + 2c_{HPO_4^{2-}} + 3c_{PO_4^{3-}} = c_{TP} \frac{K_4(c_{H^+})^2 + 2K_4K_5c_{H^+} + 3K_4K_5K_6}{(c_{H^+})^3 + K_4(c_{H^+})^2 + K_4K_5c_{H^+} + K_4K_5K_6} \quad (A.18)$$

Eq. (A.18) needs to be added to the right-hand side of Eq. (A.12) and the resulting expression for c_{alk} can be used to compute pH (i.e., c_{H^+}) as a function of TIC, TAN, TP, and alkalinity. The phosphoric acid concentration is then given by:

$$c_{H_3PO_4} = c_{TP} \left(1 + \frac{K_4}{c_{H^+}} + \frac{K_4K_5}{(c_{H^+})^2} + \frac{K_4K_5K_6}{(c_{H^+})^3}\right)^{-1} \quad (A.19)$$

References

- Bandura, A.V., Lvov, S.N., 2006. The ionization constant of water over wide ranges of temperature and density. *J. Phys. Chem. Ref. Data* 35, 15–30. <https://doi.org/10.1063/1.1928231>.
- Benson, B.B., Krause, D., 1984. The concentration and isotopic fractionation of oxygen dissolved in freshwater and seawater in equilibrium with the atmosphere. *Limnol. Oceanogr.* 29, 620–632. <https://doi.org/10.4319/lo.1984.29.3.0620>.
- Bergheim, A., Fivelstad, S., 2014. Atlantic Salmon (*Salmo salar* L.) in aquaculture: Metabolic rate and water flow requirements. In: *Salmon: Biology, Ecological Impacts and Economic Importance*. Nova Publishers Inc., New York, USA, pp. 155–171 chapter 8.
- California Institute of Technology, 2021. Carbon Dioxide - Vital Signs - Climate Change: Vital Signs of the Planet. (<https://climate.nasa.gov/vital-signs/carbon-dioxide/>).
- Davidson, J., Good, C., Williams, C., Summerfelt, S.T., 2017. Evaluating the chronic effects of nitrate on the health and performance of post-smolt Atlantic salmon *Salmo salar* in freshwater recirculation aquaculture systems. *Aquac. Eng.* 79, 1–8. <https://doi.org/10.1016/J.AQUAENG.2017.08.003>.
- FAO, 2020. The State of World Fisheries and Aquaculture 2020. Technical Report. Rome.
- Global Salmon Initiative, 2020. About Salmon Farming. (<https://globalsalmoninitiative.org/en/about-salmon-farming/>).
- Gustafsson, T.K., Waller, K.V., 1983. Dynamic modeling and reaction invariant control of pH. *Chem. Eng. Sci.* 38, 389–398. [https://doi.org/10.1016/0009-2509\(83\)80157-2](https://doi.org/10.1016/0009-2509(83)80157-2).
- Henson, M.A., Seborg, D.E., 1994. Adaptive nonlinear control of a pH neutralization process. *IEEE Trans. Control Syst. Technol.* 2, 169–182.

- Hindmarsh, A.C., Brown, P.N., Grant, K.E., Lee, S.L., Serban, R., Shumaker, D.E., Woodward, C.S., 2005. SUNDIALS: Suite of nonlinear and differential/algebraic equation solvers. *ACM Trans. Math. Softw.* 31, 363–396. <https://doi.org/10.1145/1089014.1089020>.
- Johansson, O., Wedborg, M., 1980. The ammonia-ammonium equilibrium in seawater at temperatures between 5 and 25°C. *J. Solut. Chem.* 9, 37–44. <https://doi.org/10.1007/BF00650135>.
- Khan, J.R., Johansen, D., Skov, P.V., 2018. The effects of acute and long-term exposure to CO₂ on the respiratory physiology and production performance of Atlantic salmon (*Salmo salar*) in freshwater. *Aquaculture* 491, 20–27. <https://doi.org/10.1016/J.AQUACULTURE.2018.03.010>.
- Malone, R.F., Bergeron, J., Cristina, C.M., 2006. Linear versus Monod representation of ammonia oxidation rates in oligotrophic recirculating aquaculture systems. *Aquac. Eng.* 34, 214–223. <https://doi.org/10.1016/J.AQUAENG.2005.08.005>.
- Millero, F.J., Huang, F., 2009. The density of seawater as a function of salinity (5 to 70 g kg⁻¹) and temperature (273.15 to 363.15 K). *Ocean Sci.* 5, 91–100. <https://doi.org/10.5194/os-5-91-2009>.
- Millero, F.J., Graham, T.B., Huang, F., Bustos-Serrano, H., Pierrot, D., 2006. Dissociation constants of carbonic acid in seawater as a function of salinity and temperature. *Mar. Chem.* 100, 80–94. <https://doi.org/10.1016/j.marchem.2005.12.001>.
- Mota, V.C., Nilsen, T.O., Gerwins, J., Gallo, M., Ytteborg, E., Baeverfjord, G., Kolarevic, J., Summerfelt, S.T., Terjesen, B.F., 2019. The effects of carbon dioxide on growth performance, welfare, and health of Atlantic salmon post-smolt (*Salmo salar*) in recirculating aquaculture systems. *Aquaculture* 498, 578–586. <https://doi.org/10.1016/j.aquaculture.2018.08.075>.
- Pedersen, S., Wik, T., 2020. A comparison of topologies in recirculating aquaculture systems using simulation and optimization. *Aquac. Eng.* 89, 102059. <https://doi.org/10.1016/j.aquaeng.2020.102059>.
- Raouf, J.O., 2016. Methods for determining the activity of nitrifying bacteria in wastewater samples. Ph.D. thesis. University of Stavanger.
- Schreier, H.J., Mirzoyan, N., Saito, K., 2010. Microbial diversity of biological filters in recirculating aquaculture systems. *Curr. Opin. Biotechnol.* 21, 318–325. <https://doi.org/10.1016/j.copbio.2010.03.011>.
- Summerfelt, S.T., Vinci, B.J., Piedrahita, R.H., 2000. Oxygenation and carbon dioxide control in water reuse systems. *Aquac. Eng.* 22, 87–108. [https://doi.org/10.1016/S0144-8609\(00\)00034-0](https://doi.org/10.1016/S0144-8609(00)00034-0).
- Tal, Y., Schreier, H.J., Sowers, K.R., Stubblefield, J.D., Place, A.R., Zohar, Y., 2009. Environmentally sustainable land-based marine aquaculture. *Aquaculture* 286, 28–35. <https://doi.org/10.1016/J.AQUACULTURE.2008.08.043>.
- Thorarensen, H., Farrell, A.P., 2011. The biological requirements for post-smolt Atlantic salmon in closed-containment systems. *Aquaculture* 312, 1–14. <https://doi.org/10.1016/J.AQUACULTURE.2010.11.043>.
- Vinci, B.J., Timmons, M.B., Summerfelt, S.T., Watten, B.J., 1996. Carbon Dioxide Control in Intensive Aquaculture: Design Tool Development, In: *Aquacultural Engineering Society Proceedings*, 226–244.
- Weiss, R.F., 1974. Carbon dioxide in water and seawater: the solubility of a non-ideal gas. *Mar. Chem.* 2, 203–215. [https://doi.org/10.1016/0304-4203\(74\)90015-2](https://doi.org/10.1016/0304-4203(74)90015-2).
- Wik, T.E., Lindén, B.T., Wramner, P.I., 2009. Integrated dynamic aquaculture and wastewater treatment modelling for recirculating aquaculture systems. *Aquaculture* 287, 361–370. <https://doi.org/10.1016/j.aquaculture.2008.10.056>.